

Can Uncertainty Quantification Enable Better Learning-based Index Tuning?

Tao Yu, Zhaonian Zou, Hao Xiong

Abstract—Index tuning is crucial for optimizing database performance by selecting optimal indexes based on workload. The key to this process lies in an accurate and efficient benefit estimator. Traditional methods relying on what-if tools often suffer from inefficiency and inaccuracy. In contrast, learning-based models provide a promising alternative but face challenges such as instability, lack of interpretability, and complex management. To overcome these limitations, we adopt a novel approach: quantifying the uncertainty in learning-based models' results, thereby combining the strengths of both traditional and learning-based methods for reliable index tuning. We propose BEAUTY, the first uncertainty-aware framework that enhances learning-based models with uncertainty quantification and uses what-if tools as a complementary mechanism to improve reliability and reduce management complexity. Specifically, we introduce a novel method that combines AutoEncoder and Monte Carlo Dropout to jointly quantify uncertainty, tailored to the characteristics of benefit estimation tasks. In experiments involving sixteen models, our approach outperformed existing uncertainty quantification methods in the majority of cases. We also conducted index tuning tests on six datasets. By applying the BEAUTY framework, we eliminated worst-case scenarios and more than tripled the occurrence of best-case scenarios.

Index Terms—Index tuning, database, benefit estimation, uncertainty quantification.



1 INTRODUCTION

Indexes are a crucial means for accelerating database queries. However, poorly configured indexes not only waste storage resources but can also degrade system performance. The automatic creation of suitable indexes has long been a major research focus, commonly referred to as index tuning [1], [2]. The component that addresses this challenge, known as the index advisor, typically consists of two parts. The first is the index configuration enumerator, which continuously generates potential index configurations. These configurations are then passed to the second component, the benefit estimator, responsible for estimating the benefits these index configurations would bring to the workload, without actually creating the indexes.

Benefit estimation (BE) plays a critical role in effective index tuning. The most common method involves using *what-if tools* [3] to create virtual indexes and utilizing the query optimizer to estimate their potential benefits. However, this approach has two significant drawbacks: (1) **Low inference efficiency**: The optimizer needs to sequentially compare the costs of almost all execution plans of a query. This process accounts for nearly 90 percent of the entire index tuning time [4]. (2) **Low accuracy**: The optimizer's cardinality and cost estimators often produce significant errors, especially for complex queries.

To address these issues, researchers have studied learning-based models for benefit estimation, such as [5], [6], [7]. While these models generally improve efficiency,

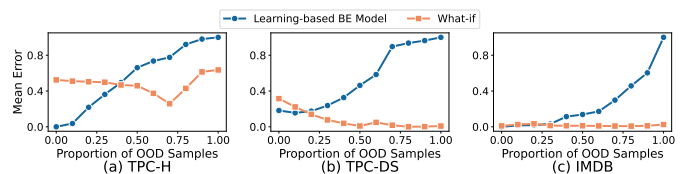


Fig. 1: Mean errors of a learning-based BE model and a what-if tool.

they present new challenges when deployed in real-world systems.

(1) **Poor stability**: Learning-based models typically outperform what-if tools on data similar to their training sets, but they can generate highly erroneous results when query patterns shift or training data is insufficient. As shown in Figure 1, we compare a learning-based BE method with a what-if tool on varying proportions of out-of-domain (OOD) samples. When the proportion reaches around 25%, the mean errors of two methods are comparable, but the mean error of the learning-based method becomes larger than the what-if tool as the OOD sample proportion increases.

(2) **Lack of interpretability**: Learning-based models are often black-box systems, making them difficult to understand when and why they perform poorly in real-world applications.

(3) **Complex management**: These models require extensive data collection before deployment and ongoing monitoring to determine when updates are necessary, adding considerable overhead.

Due to the poor stability of learning-based models, some estimation results will inevitably be highly inaccurate and unreliable, leading the index advisor to select suboptimal indexes. Furthermore, the lack of interpretability prevents us from determining when or why the model produces unreliable results, making it difficult to fundamentally address the stability issue. In this paper, we propose a different

- Tao Yu is a Ph.D. student at Harbin Institute of Technology, P.R. China. Email: 21B903056@stu.hit.edu.cn.
- Zhaonian Zou is with the School of Computer Science and Technology, Harbin Institute of Technology, P.R. China. Email: znzou@hit.edu.cn. Corresponding author.
- Hao Xiong is a Master's degree student at Harbin Institute of Technology, P.R. China.

approach by quantifying the uncertainty of the model’s results through specific metrics. When the model’s estimate for a test sample shows high uncertainty, the result is more likely to significantly deviate from the true value. This technique, known as uncertainty quantification (UQ), has been widely studied in fields where model errors have serious consequences, such as medical image detection [8], autonomous driving [9], and drug analysis [10].

By using this approach, we can return only the reliable benefit estimation results to the index advisor, while utilizing what-if tools to obtain the remaining results, thereby improving the reliability of the BE module. To achieve this, we propose the first uncertainty-aware BE framework, named BEAUTY (**benefit estimation with uncertainty**). It employs UQ techniques to combine the strengths of learning-based BE models and what-if tools, ensuring compatibility with existing systems. Additionally, by monitoring the proportion and causes of uncertain results during model runtime, we can determine when to update the model, reduce model management costs, and guide model design. We believe this framework will facilitate the broader adoption of learning-based models.

Although many UQ methods are designed for general tasks, their accuracy and efficiency are suboptimal when applied directly to BE tasks. To address this, we conducted a systematic study of the sources of uncertainty in learning-based BE models and performed a finer-grained analysis. Based on our findings, we propose a novel hybrid UQ method that integrates AutoEncoder and Monte Carlo Dropout into existing BE models. This method aligns with the structure of current learning-based estimators and outperforms general-purpose UQ methods in most scenarios. Additionally, we introduce a scheme that balances quantification accuracy and inference efficiency, tailored to the specific characteristics of the model. The source code and data for this study are available at ¹.

In summary, this paper makes the following contributions:

(1) We conducted a systematic study of the sources of uncertainty in learning-based BE models within the context of index tuning. Based on the characteristics of these tasks, we proposed a novel hybrid UQ method that allows for a flexible trade-off between efficiency and accuracy, depending on the specific characteristics of the BE task (Section 4). Our experiments demonstrate that the proposed UQ method outperforms general-purpose UQ methods in five out of six scenarios.

(2) We introduced BEAUTY, the first uncertainty-aware BE framework, which combines the strengths of learning-based models with what-if tools, enabling uncertainty-driven model updates. Our experiments across six benchmarks with varying budgets show that the BEAUTY framework significantly improves index tuning performance (Section 6).

(3) In our experiments, we applied existing UQ methods to various learning-based BE models, creating a total of 16 different models (Section 5). We thoroughly evaluated the impact of these methods on model accuracy and efficiency, confirming the superiority of our proposed UQ method.

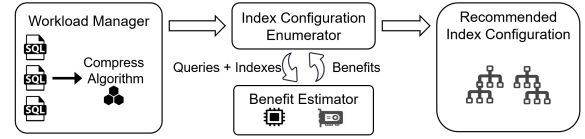


Fig. 2: Typical structure of index advisors.

2 BACKGROUND

2.1 Index Advisors

Index advisors are responsible for index tuning, that is, recommending indexes for databases [11]. The typical process of index tuning is illustrated in Figure 2. An index advisor consists of three critical modules.

Workload Manager: The workload manager periodically collects a set of queries $\{q_1, q_2, \dots, q_n\}$ recently executed under the current index configuration \mathcal{I}_0 created on the database. The queries, along with their execution plans and weights (indicating frequencies or importance) $w_i \in \mathbb{R}$, form a workload W .

Index Configuration Enumerator: The index configuration enumerator generates potential index configurations \mathcal{I} that aim to reduce the execution time of W subject to the budget constraint such as the maximum storage space of \mathcal{I} . There are mainly two approaches to enumerating index configurations. The early research primarily focused on greedy algorithms [12], [13], [14] or linear programming [15]. The other approach models the problem as a reinforcement learning task, employing techniques such as Monte Carlo Tree Search [4], Multi-Armed Bandit [16], [17], or Deep Reinforcement Learning [18], [19].

Benefit Estimator: Let $c(q, \mathcal{I})$ denote the cost of executing query q with the support of index configuration \mathcal{I} . The *benefit* of replacing \mathcal{I}_0 with \mathcal{I} for query q is defined as $B(q, \mathcal{I}_0, \mathcal{I}) = c(q, \mathcal{I}_0) - c(q, \mathcal{I})$. For each enumerated configuration \mathcal{I} , the benefit estimator computes the estimated benefit of executing all queries in the workload W without actually building the indexes in \mathcal{I} .

The index configuration enumerator and the benefit estimator operate interactively. Eventually, the index configuration \mathcal{I} that maximizes the overall benefit

$$B(W, \mathcal{I}_0, \mathcal{I}) = \sum_{i=1}^n w_i \cdot B(q_i, \mathcal{I}_0, \mathcal{I}). \quad (1)$$

is recommended for the database. Clearly, maximizing $B(W, \mathcal{I}_0, \mathcal{I})$ is equivalent to minimizing the total cost $c(W, \mathcal{I}) = \sum_{i=1}^n w_i \cdot c(q_i, \mathcal{I})$.

2.2 Learning-based Benefit Estimation (BE) Models

The benefit estimator plays a crucial role in index tuning as its efficiency directly impacts the overall performance of index tuning, and its accuracy affects the behavior of the index configuration enumerator [15], [20], [21]. Traditionally, what-if tools have been used to create hypothetical indexes, and the query optimizer is employed to estimate the total cost $c(W, \mathcal{I})$. However, due to their inefficiency and inaccuracy, particularly, for complex queries, machine learning (ML) techniques have been recently introduced to develop faster and more accurate BE models. One approach such as DISTILL [1] involves training multiple lightweight BE models for each query template to collectively estimate benefits. The other approach is to train a single complex

1. <https://github.com/HIT-DB-Group/Beauty>

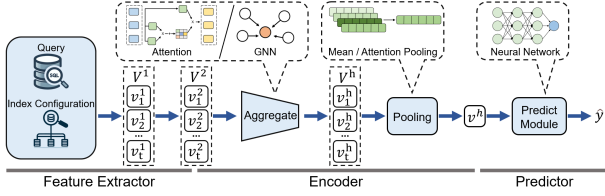


Fig. 3: The typical architecture of a learning-based BE model.

BE model using historical query execution data, either to completely replace the what-if tool or to adjust the outputs of the what-if tool. The latter approach is the main focus of our study. LIB [7] and AMA [6] are notable examples of this approach. As shown in Figure 3, the typical architecture of a learning-based BE model consists of three modules.

Feature Extractor: The feature extractor represents the information relevant to the BE model as a set of vectors for processing. The encoded information includes the index configuration \mathcal{I} , the SQL statement of query q , the query plan of q under the current index configuration \mathcal{I}_0 , the database schema, the database statistics, the hardware environment, and so on. According to the data type, each feature can be classified as numerical or categorical. The features are encoded into a set of vectors $V^1 = \{v_1^1, v_2^1, \dots, v_t^1\}$. Depending on the model design, the number t of vectors in V^1 can be fixed (e.g., AMA [6]) or variable (e.g., LIB [7]) for different queries and environments. For each vector v_i^1 , the elements encoding the categorical features are replaced by higher-dimensional vectors using one-hot encoding or learnable word embedding, resulting in a vector v_i^2 with higher dimensionality than v_i^1 . Thus, the input vector set for the BE model is $V^2 = \{v_1^2, v_2^2, \dots, v_t^2\}$.

Hidden Vector Encoder: Each vector in V^2 represents an aspect of the information relevant to the BE model. Since the vectors in V^2 are often sparse, they are usually consolidated into a compact and information-rich hidden vector v^h . If the number of vectors in V^2 varies across queries, a recurrent neural network (RNN), a graph neural network (GNN), or the multi-head attention mechanism can be used as the encoder for v^h , allowing each vector $v_i^2 \in V^2$ to interact with other vectors $v_j^2 \in V^2$. It first produces an intermediate representation $V^h = \text{Aggregate}(V^2) = \{v_1^h, v_2^h, \dots, v_t^h\}$, and then, the vectors in V^h are processed into the final hidden vector $v^h = \text{Pool}(V^h)$ using techniques such as pooling or adding a super node. If the number of vectors in V^2 is fixed, a multi-layer perceptron (MLP) is often used as the encoder for the hidden vector, i.e., $v^h = \text{MLP}(V^2)$.

Predictor: The predictor, typically a MLP, takes the hidden vector v^h as input and generates the final output $\hat{y} = \text{MLP}(v^h)$ which represents an estimate of either $c(q, \mathcal{I})$ or $B(q, \mathcal{I}_0, \mathcal{I})$.

2.3 Uncertainty in Machine Learning (ML) Models

Uncertainty is the quality or state of being uncertain, which arises in every stage of a ML task, including data acquisition, feature encoding, model design, model training, and model inference [22]. Naturally, uncertainty is inherent in ML-based index tuning, which will be explained in subsection 4.2. As illustrated in Figure 4, there are two different types of uncertainty, often referred to as *aleatoric uncertainty* and *epistemic uncertainty* [23].

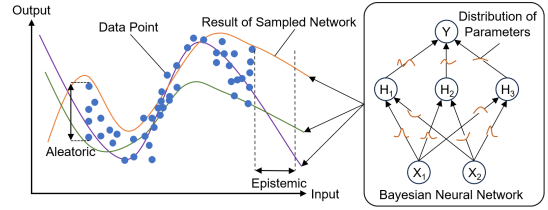


Fig. 4: A set of data points and a Bayesian neural network (BNN) trained based on them. The curves on the left represent the fitting curves for three different neural network samples from the BNN. The relationships between these curves and the data points demonstrate the distinction between aleatoric and epistemic uncertainty.

Aleatoric uncertainty, also known as *data uncertainty* or *statistical uncertainty*, refers to the notion of randomness, that is, the variability in the outcome of an experiment (i.e., random errors) caused by inherently random effects. For instance, the data collected by sensors usually has aleatoric uncertainty because the same input target might correspond to different sensing outputs at random. In principle, aleatoric uncertainty cannot be reduced by incorporating additional information such as collecting more data or using better models [24]. Aleatoric uncertainty can be further divided into *homoscedastic* and *heteroscedastic* depending on if the inherent randomness varies with the input target.

Epistemic uncertainty, also known as *model uncertainty* or *systematic uncertainty*, refers to uncertainty caused by the ignorance of knowledge (about the best model). Epistemic uncertainty may result in errors generated in the design, training and inference of a model. For example, if the inference of a model is made on a dataset that has a distribution significantly different from the model’s training dataset, the model might provide inaccurate outputs due to ignorance. As opposed to uncertainty due to randomness, uncertainty caused by ignorance can in principle be reduced based on additional information. In other words, epistemic uncertainty refers to the reducible part of the (total) uncertainty, whereas aleatoric uncertainty refers to the irreducible part.

Uncertainty Quantification (UQ): A number of model-independent and model-dependent methods have been proposed to quantify the two types of uncertainty. The first category includes Bayesian neural networks (BNNs) [25], [26], Monte Carlo dropout (MCD) methods [27], and ensemble methods [28], [29], which do not rely on the specific models in which the uncertainty is quantified. The second category incorporates UQ into model-specific structures. For example, HSTO [30] replaces the multi-head attention mechanism with hierarchical stochastic self-attention to achieve UQ. In this paper, we will reproduce these methods in the experimental evaluation and compare them with our proposed hybrid UQ approach.

3 PROBLEM

Since collecting training data is costly, ML models inevitably encounter out-of-distribution (OOD) data, leading to unreliable outputs. The unreliable results produced by learning-based benefit estimators can lead index advisors to select inappropriate indexes, significantly degrading database performance. Therefore, as discussed in section 1, we will explore how UQ techniques can be leveraged to determine

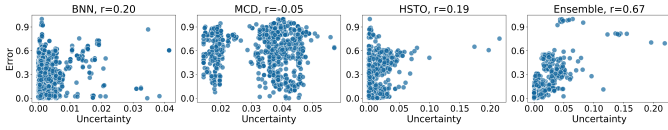


Fig. 5: Joint distribution of model error and model uncertainty evaluated using UQ methods BNN [31], MCD [27], HSTO [30], and Ensemble [32]. r : Pearson’s correlation coefficient.

whether the results produced by learning-based BE models are reliable and how to integrate uncertainty-aware benefit estimators into index advisors. Specifically, this paper addresses the following three key research questions:

Q1: How can the uncertainty in a learning-based BE model be precisely quantified? Accurately quantifying the uncertainty in a learning-based BE model presents a significant challenge, and directly applying the existing methods often yields suboptimal performance. As shown in Figure 5, on a OOD dataset, model error and model uncertainty are generally not highly linearly correlated, that is, a large model error may not mean large model uncertainty. In this paper, the first problem is how to precisely quantify the uncertainty in a learning-based BE model. Rather than applying the existing general-purpose UQ methods directly, we propose a hybrid quantification method in section 4 tailored to the unique characteristics of the BE problem, providing more precise quantification of uncertainty than the general-purpose methods.

Q2: What impacts does UQ have on a BE model? In section 5, we will conduct an empirical study to understand the impacts of UQ on BE models by evaluating the accuracy, training cost, and inference cost of the BE models enhanced with UQ. In subsection 4.4, we will also explore a new method for determining when a BE model needs to be updated based on quantified uncertainty.

Q3: What impacts does a UQ-enhanced BE model have on the index advisor? In section 6, we will evaluate 8 UQ-enhanced BE models with 6 workloads across 36 scenarios to investigate the effects of the accuracy and efficiency of UQ on the index advisor.

Due to space constraints, we focus exclusively on BE models based on neural networks (NNs). NN-based models have been receiving increasing attention and generally achieve higher accuracy. The approach proposed in this paper can be easily extended to non-NN models by replacing the UQ methods for non-NN models such as [33], [34].

4 THE BEAUTY FRAMEWORK

To answer the questions in section 3, we propose our new framework for benefit estimation called BEAUTY (Benefit estimation with uncertainty).

4.1 Overview

The process of index tuning with BEAUTY is illustrated in Figure 6. After generating an index configuration by the enumerator, the advisor uses the uncertainty-aware learning-based BE model to estimate both the benefits that the configuration brings to the queries in the workload and the confidence levels of the estimated benefits. Then, the result filter examines the estimated benefits and their uncertainty with respect to a specified uncertainty threshold. The

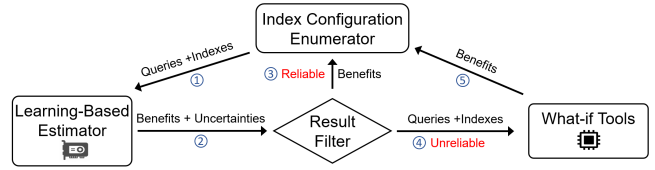


Fig. 6: The index tuning process with BEAUTY.

TABLE 1: Five categories of uncertainty in learning-based BE models.

Category	Type	Cause	Module for Quantification
U1	Epistemic	Insufficient information modeling	Predictor
U2	Epistemic	Flawed feature extraction	Predictor
U3	Epistemic	Inadequate model design and training	Hidden Vector Encoder
U4	Epistemic	Insufficient training data	Hidden Vector Encoder
U5	Aleatoric	Randomness in query execution time	Predictor

estimated benefits with uncertainty below the threshold are deemed reliable and are returned to the enumerator. For the remaining estimated benefits on which the BE model has low confidence due to insufficient training data or feature extraction deficiencies, the what-if tool that is usually more robust than learning-based BE models are invoked instead for benefit estimation.

4.2 Uncertainty in Learning-based BE Models

The existing UQ methods are designed for general ML models and scenarios, lacking specific knowledge necessary for benefit estimation. To overcome this limitation, we propose a hybrid UQ method tailored to the unique characteristics of the BE problem, providing more precise quantification of uncertainty than the general-purpose methods. To this end, we conduct the first analysis of the sources of uncertainty in the BE problem and their relationships to the structures of learning-based BE models, which lays foundations for designing the uncertainty-aware BE model in BEAUTY.

Uncertainty emerges throughout the whole process of learning-based BE models from design to training and to inference. We divide the uncertainty into five categories which are summarized in Table 1.

U1: Epistemic uncertainty due to insufficient information modeling. Estimating the benefit of an index configuration for a query is a complex task, as it requires invoking the query optimizer to retrieve the plans of the query before and after creating the indexes in the configuration. Existing learning-based estimators only model the information most relevant to this query such as the index configuration, the current query plan, and the plan chosen by the optimizer after virtually creating the indexes in the configuration. However, some overlooked factors can also significantly affect query execution costs. One such factor is data distributions which determine the cardinalities of intermediate results produced during the execution of a query. Existing learning-based estimators either do not model data distributions or model them in an over-simplified manner. Cardinality estimation itself is challenging and is a key research focus in the AI4DB field. State-of-the-art data-driven cardinality estimation methods are often built on deep-learning models which are more complex than those used in the existing BE models. Another factor that significantly affects query execution costs is the configuration of the database system such as the knobs `work_mem` and `shared_buffers`. Finally, the implementation of the query optimizer itself can alter the selected plan for a query and varies its execution cost.

Currently, none of the learning-based estimators has taken all these relevant information into account. The ignorance of these information leads to epistemic uncertainty.

U2: Epistemic uncertainty caused by flawed feature extraction. Learning-based BE models require encoding various BE-related information into vectors, e.g., query statements, query plans, indexes, and database states. Incomplete encoding process may cause information loss. Moreover, flawed feature extraction techniques may represent different training samples into the same vector, resulting in a training set where the same sample attain conflicting labels, thus contributing to epistemic uncertainty.

U3: Epistemic uncertainty due to inadequate model design and training. A ML model's expression power is limited by its structure and adopted mechanisms, as well as the settings of the hyperparameters and training process, e.g., batch size, optimization algorithm, learning rate, and stopping criteria. As a result, even on the training data, the model cannot be 100% accurate in general. The portion of the data that the model fails to fit yields epistemic uncertainty.

U4: Epistemic uncertainty caused by insufficient training data. Training a BE model requires collecting the execution plans and costs of a set of queries under different index configurations, which places a heavy burden on the system. Additionally, the collected data might not cover all application scenarios, and therefore, out-of-domain (OOD) issues often occur during inference. For instance, if a BE model was trained mostly with OLAP queries but is applied mostly to OLTP queries during inference, the model's accuracy tends to decline in practice.

U5: Aleatoric uncertainty due to the randomness in query execution time. Due to physical factors such as caching, system resource scheduling, and hardware conditions, the execution time of a query is not fixed but a random variable within a certain range. Therefore, if a BE model estimates benefits based on observed query execution time, the model's outputs must exhibit randomness, and the randomness is related to the characteristics of queries, resulting in heteroscedastic aleatoric uncertainty.

4.3 Hybrid Quantification Method

In this section, we propose a hybrid method for quantifying uncertainty in a learning-based BE model. We first describe which modules in the BE model is each category of uncertainty mainly quantified from, followed by the design of specific quantification methods.

4.3.1 Modules for Quantifying Uncertainty

As described in subsection 2.2, there are three main modules in a learning-based BE model: the feature extractor, the hidden vector encoder, and the predictor. Here, we analyze the relationship between the five categories of uncertainty listed in subsection 4.2 and the modules of the BE model, which lays the foundation for our hybrid UQ method.

Quantifying Uncertainty from Hidden Vector Encoder Module. Uncertainty U3 and U4 arise from limited model capacity and insufficient data, leading to the discrepancy between the benefit function fitted by the model and the true benefit function. Uncertainty U3 and U4 are unrelated to the feature extractor. The hidden vector encoder and the predictor are responsible for the mapping process, with the hidden

vector encoder being the key module that determines the model's fitting ability. It transforms rich, high-dimensional information into a low-dimensional space, and the quality of the hidden feature vector \mathbf{v}^h it produces directly reflects the model's ability to fit the benefit function. Consequently, uncertainty U3 and U4 is quantified in the hidden vector encoder module.

Quantifying Uncertainty from Predictor Module. Due to the presence of U5, the output of the BE model exhibits randomness. However, the current benefit estimator produces a fixed estimated benefit value given a fixed input q, \mathcal{I}_0 and \mathcal{I} , so we need to modify the BE model to make its output random, with a distribution as close as possible to the true benefit distribution. Among the two modules responsible for the mapping process, the hidden vector encoder primarily removes redundant information and extracts features, and it has already been used to quantify uncertainty U3 and U4. Therefore, the task of introducing randomness into the output is assigned to the predictor module which directly generates the output. Consequently, uncertainty U1, U2, and U5 is quantified in the predictor.

Uncertainties U1 and U2 arise from deficiencies in the feature extractor: some data with different benefits $B(q, \mathcal{I}_0, \mathcal{I})$ result in identical input vectors V^1 for the model. For the model, this still implies that the output exhibits randomness, i.e., the same input corresponds to multiple possible outputs. Thus, uncertainty U1 and U2 can also be quantified within the predictor module.

4.3.2 Quantifying Uncertainty from Hidden Vector Encoder

Given a learning-based BE model, uncertainties U3 and U4 represent the model's fitting error with respect to the benefit function f , which is reflected in the quality of the hidden feature vector \mathbf{v}^h extracted by the hidden vector encoder module. To evaluate the quality of \mathbf{v}^h , we employ the well-known concept of *AutoEncoder* [35] and incorporate a decoder network structure into the BE model. The basic idea is as follows. The added decoder tries to reconstruct the input V^1 of the hidden vector encoder from the intermediate representation V^h , i.e., $\hat{V}^1 = Decoder(V^h) = \{\hat{\mathbf{v}}_1^1, \hat{\mathbf{v}}_2^1, \dots, \hat{\mathbf{v}}_t^1\}$. The quality of the reconstruction is assessed by the total mean squared error (MSE) between all pairs of corresponding vectors $\mathbf{v}_i \in V^1$ and $\hat{\mathbf{v}}_i \in \hat{V}^1$, that is,

$$\mathcal{U}_1 = \frac{1}{t} \sum_{i=1}^t MSE(\mathbf{v}_i^1, \hat{\mathbf{v}}_i^1). \quad (2)$$

\mathcal{U}_1 quantifies the uncertainty in the BE model with respect to the input V^1 of the hidden vector encoder module.

The rationale behind this approach lies in the fact that for the decoder to accurately reconstruct V^1 from V^h , two essential conditions must be satisfied. First, the structure of the hidden vector encoder must be appropriate. The network structure of the decoder should be symmetric to that of the encoder. Only if the encoder's structure can gradually eliminate unimportant features and reduce dimensionality, the decoder can reverse this process and reconstruct V^1 based on the essential features. Second, the quality of the latent representation V^h must be high. Given that the structure of the decoder is appropriate, the quality of the decoder's input also determines the quality of the reconstruction. Therefore, when the divergence between V^1 and \hat{V}^1 is very

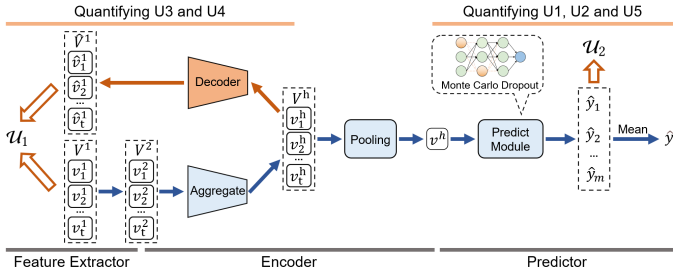


Fig. 7: The BEAUTY framework for joint benefit estimation and uncertainty quantification.

small, the encoder has processed V^1 effectively, indicating low uncertainty in the hidden vector encoder module.

As depicted in Figure 7, the encoder transforms V^2 to \mathbf{v}^h , but the decoder transforms V^h to \hat{V}^1 . Obviously, the encoder and the decoder do not carry out strictly inverse processes. First, V^h is used as the input of the decoder rather than \mathbf{v}^h . This is because the pooling in the encoder that transforms V^h to \mathbf{v}^h irreversibly compresses most information, e.g., the number of vectors in V^h . The loss of information makes subsequent reconstruction in the decoder impossible. Second, V^1 is set as the target of the reconstruction process carried out by the decoder instead of V^2 . This is because after transforming the categorical features in the vectors in V^1 to embeddings, the sparsity of the vectors increases, and the richness of information decreases, which significantly increases the difficulty in reconstruction carried out by the decoder. Our experiments verify that the design of the decoder is reasonable and effective.

In Eq. (2), the MSE between \mathbf{v}_i^1 and $\hat{\mathbf{v}}_i^1$ is computed, where all elements of \mathbf{v}_i^1 and $\hat{\mathbf{v}}_i^1$ are considered equally important. However, in practice, different features can have different impacts on BE, and important features can be assigned higher weights. In engineering practice, MSE can be replaced by weighted MSE, and the practitioners can properly set weights to the dimensions of \mathbf{v}_i^1 and $\hat{\mathbf{v}}_i^1$.

4.3.3 Quantifying Uncertainty from Predictor

After using the decoder to quantify uncertainty U3 and U4 in the hidden vector encoder, we proceed to quantify uncertainties U1, U2, and U5 in the predictor module. To ensure compatibility with the existing benefit estimator, we cannot assume that the model adopts specialized mechanisms, such as GNN or multi-head attention. Thus, considering the available UQ methods [22], we have two options:

(1) *Bayesian Neural Networks (BNNs)*. BNNs have been extensively studied for UQ. Let \mathcal{N} be a neural network (NN). To quantify the uncertainty in \mathcal{N} , a BNN \mathcal{B} is induced, which has the same structure as \mathcal{N} but treats each parameter w in \mathcal{N} as a random variable X_w following a probability distribution. Let W be the set of all parameters in \mathcal{N} and $\mathbf{X}_W = \{X_w \mid w \in W\}$ be the set of corresponding random variables in \mathcal{B} . Given a training set $D = \{(\mathbf{x}_i, y_i) \mid 1 \leq i \leq n\}$, the goal is to learn the posterior probability density function $p(\mathbf{X}_W|D)$, which is given by

$$\begin{aligned} p(\mathbf{X}_W|D) &= \frac{p(D|\mathbf{X}_W)p(\mathbf{X}_W)}{p(D)} \\ &= \frac{p(D|\mathbf{X}_W)p(\mathbf{X}_W)}{\int \cdots \int p(D|\mathbf{X}_W)p(\mathbf{X}_W)d\mathbf{X}_W}. \end{aligned}$$

The prior distribution $p(\mathbf{X}_W)$ should reflect prior beliefs about the distribution of the weights W before observing

any data. Solving this equation directly can be challenging, so *variational inference (VI)* is often employed [36], [26]. Blundell et al. [31] proposed the renowned *Bayes by Backprop (BBB)* algorithm, which is compatible with backpropagation and facilitates learning a probability distribution. We select the BBB algorithm as the baseline in the subsequent experimental evaluation.

The trained BNN \mathcal{B} and its inference process are depicted in Figure 4. The uncertainty in the NN \mathcal{N} with respect to a test record \mathbf{x} is assessed as follows. First, a collection of parameter settings $\{W_1, W_2, \dots, W_m\}$ is obtained through independent Monte Carlo sampling from the posterior distribution $p(\mathbf{X}_W|D)$. By setting the parameters W to each sampled configuration W_i , a specific instance \mathcal{N}_i of \mathcal{N} is obtained. Given the test record \mathbf{x} as input, let y_i be the output of \mathcal{N}_i . The mean of $\hat{y}_1, \hat{y}_2, \dots, \hat{y}_m$ is the prediction for \mathbf{x} , and the variance of $\hat{y}_1, \hat{y}_2, \dots, \hat{y}_m$ is the uncertainty of \mathcal{N} with respect to \mathbf{x} . In practice, the sampling and inference processes can be combined and performed in an interleaved, layer-by-layer manner on \mathcal{N} .

(2) *Monte Carlo Dropout (MCD) Methods*. *Dropout* layers are commonly used in deep NNs to prevent overfitting. During training, a dropout layer randomly sets elements of the input tensor to 0 with probability $p \in [0, 1]$ and scales up the remaining elements by $1/(1-p)$ to maintain the sum over all inputs. The zeroed elements are chosen independently for each forward pass. During inference, dropout layers are typically disabled. However, to represent model uncertainty, dropout layers can be activated during inference. Gal and Ghahramani [27] proved that dropouts can approximate Bayesian inference in BNNs. Given a test record \mathbf{x} , model inference is repeated multiple times independently, yielding outputs $\hat{y}_1, \hat{y}_2, \dots, \hat{y}_m$. The mean of these outputs is the prediction for \mathbf{x} , and the variance represents the model's uncertainty with respect to \mathbf{x} .

In the BE scenario, we prefer the MCD method over BNNs for two reasons. First, BNNs require more extensive modifications to the BE model compared to MCD. Second, the training cost of a BNN is usually higher because BNNs often require multiple parameters to represent the distribution of a single neuron parameter. For instance, if a neuron's weight follows a normal distribution $N(\mu, \sigma)$, two parameters, μ and σ , are needed to characterize the distribution. Thus, a BNN requires significantly more parameters than a standard NN, leading to increased training costs.

Specifically, we introduce MCD into the original MLP of the Predictor to approximate BNNs. After the encoder produces the hidden representation \mathbf{v}^h , a set of predictions $\{\hat{y}_1, \hat{y}_2, \dots, \hat{y}_m\}$ is generated by the approximated BNNs, i.e., $\{\hat{y}_1, \hat{y}_2, \dots, \hat{y}_m\} = MLP_{MCD}(\mathbf{v}^h)$. The mean of $\hat{y}_1, \hat{y}_2, \dots, \hat{y}_m$ is returned as the prediction for $B(q, \mathcal{I}_0, \mathcal{I})$, and the uncertainty is quantified as

$$\mathcal{U}_2 = \text{Var}(\hat{y}_1, \hat{y}_2, \dots, \hat{y}_m). \quad (3)$$

4.3.4 Result Filter

Once the BE model with UQ capability (referred to as the BE-UQ model) provides the estimated benefit \hat{y} and the quantified uncertainties \mathcal{U}_1 and \mathcal{U}_2 , the Result Filter module (as shown in Figure 6) determines whether \hat{y} should be returned to the Estimator.

Thresholds θ_1 and θ_2 are predefined for \mathcal{U}_1 and \mathcal{U}_2 , serving as reliability indicators. If \mathcal{U}_1 exceeds the threshold

θ_1 —associated with uncertainties U3 and U4—this suggests that $\hat{B}(q, \mathcal{I}_0, \mathcal{I})$ likely diverges significantly from true value. Similarly, if \mathcal{U}_2 exceeds θ_2 —associated with uncertainties U1, U2, and U5—this indicates that \hat{y} has a high variance. Specifically, the returned result $\hat{B}(q, \mathcal{I}_0, \mathcal{I})$ should follow:

$$\hat{B}(q, \mathcal{I}_0, \mathcal{I}) = \begin{cases} \hat{y} & \text{if } \mathcal{U}_1 \leq \theta_1 \text{ and } \mathcal{U}_2 \leq \theta_2, \\ \text{What-if tools} & \text{otherwise.} \end{cases}$$

The domain of θ_1 and θ_2 is $[0, +\infty)$, and their values vary based on factors such as model structure, hyperparameters, query workload, and the database instance. Setting fixed, universal thresholds for \mathcal{U}_1 and \mathcal{U}_2 is impractical. Therefore, we adopt a context-dependent approach to define relative thresholds θ_1 and θ_2 : for a new sample, if the model’s uncertainty regarding it is comparable to the uncertainty observed during training when the model performed optimally with minimal uncertainty, the result is deemed reliable. Specifically, after training the BE-UQ model, we perform inference for each training sample $(q, \mathcal{I}_0, \mathcal{I})$ and gather the quantified uncertainties \mathcal{U}_1 and \mathcal{U}_2 . The 90th percentile of \mathcal{U}_1 (or \mathcal{U}_2) across all training samples is designated as θ_1 (or θ_2).

4.4 Model Deployment

4.4.1 Model Training

Compared to the original BE model, our BE-UQ model incorporates two additional modules: the decoder and MCD. Since the decoder cannot be trained concurrently with the original BE model, a redesigned training process is required. In our index advisor, the BE-UQ model is trained in two distinct phases. First, the BE model—which includes the feature extractor, hidden vector encoder, and Predictor—is trained following the original BE model’s method. In the second phase, the parameters of the feature extractor and hidden vector encoder are frozen, and the decoder is trained by minimizing the MSE loss.

The rationale behind this training method is that BE remains the primary objective of the BE-UQ model, while UQ is secondary. Our approach ensures that the accuracy of the BE model is maintained, regardless of whether UQ is utilized. By preserving the accuracy of the hidden vector encoder, we ensure that the input information is effectively encoded in the intermediate representation V^h . This, in turn, enables the decoder to accurately reconstruct the input vector set \hat{V}^1 and correctly quantify uncertainty.

Although there are alternative ways to train the BE-UQ model, such as jointly training the hidden vector encoder and decoder followed by training the Predictor, this method shifts the encoder’s focus toward UQ rather than BE, which conflicts with our objectives. Therefore, our proposed training method is better suited for the index tuning task.

4.4.2 Uncertainty-Driven Model Updating

The performance of the BE-UQ model may decline when the database or query workload changes. To maintain the accuracy and stability of the model, it must be updated promptly when performance starts to decrease. There are two common ways to determine whether a machine learning model requires updating.

The first category samples predictions during model inference and compares them with actual values. A model

update is needed if the error is significantly large. However, this approach has two main drawbacks. First, the actual benefits $B(q, \mathcal{I}_0, \mathcal{I})$ for the sampled instances $(q, \mathcal{I}_0, \mathcal{I})$ must be known. To determine $B(q, \mathcal{I}_0, \mathcal{I})$, the indexes in \mathcal{I} must be created, and the query q must be executed based on those indexes, which incurs substantial time and space costs. Second, this method may cause delayed updates due to sampling errors.

The second category triggers model updates when a decrease in system efficiency is detected. However, this approach causes updates to lag behind the onset of performance regression. More importantly, in the context of index tuning, the optimal index is unknown. Even if an erroneous BE result leads to the creation of a suboptimal index, system performance may still improve slightly. Thus, it is difficult to determine whether the model requires updating based on this result.

In the BEAUTY framework, we have a more accurate and timely metric to determine whether an update is needed: if the what-if tool estimates benefits for a significant portion of test samples $(q, \mathcal{I}_0, \mathcal{I})$, this likely indicates that the BE-UQ model no longer fits the current dataset, workload, or system conditions and requires updating. Additionally, the uncertainties \mathcal{U}_1 and \mathcal{U}_2 returned by the model can help guide the update process.

(1) If the what-if tool estimates the benefits for a significant portion of test samples $(q, \mathcal{I}_0, \mathcal{I})$ due to $\mathcal{U}_1 > \theta_1$, this suggests that the BE-UQ model cannot provide effective latent vectors under the current workload. For example, if there have been substantial changes in query patterns or index configurations, the BE-UQ model may fail to produce accurate results. In this case, more data must be collected from the current workload to retrain or fine-tune the model.

(2) If the what-if tool estimates the benefits for a significant portion of test instances $(q, \mathcal{I}_0, \mathcal{I})$ due to $\mathcal{U}_2 > \theta_2$, this indicates that the BE-UQ model is unable to distinguish between too many queries and index configurations in the current workload. Due to insufficient modeling information or flaws in feature extraction, the model estimates a wide range of benefits for the same test instance, leading to unreliable predictions. In such cases, the designer must identify the missing information or flaws in feature extraction and redesign the model based on the current workload.

4.4.3 Improving Efficiency.

During index tuning, the efficiency of benefit estimation significantly affects the tuning time and, in some cases, can influence the final tuning quality, particularly with algorithms like DTA that can be interrupted at any point. Faster estimation allows for exploring more index configurations, ultimately leading to better results. Although our framework enhances the reliability of benefit estimation, it inevitably introduces additional overhead. Here, we present a more efficient version for scenarios with tight time constraints. In terms of quantification overhead, \mathcal{U}_2 incurs greater cost than \mathcal{U}_1 : the AutoEncoder requires an extra decoder inference, while MCD necessitates dozens of inferences by the Prediction Module to ensure result stability [37].

In terms of the importance of quantification, \mathcal{U}_1 is more critical than \mathcal{U}_2 : (1) Among the uncertainties affecting \mathcal{U}_2 , U1 and U2 arise from flaws in the model design. These

TABLE 2: Summary of databases and workloads and the maximum runtime for index tuning algorithm DTA.

Benchmark	DB SF/Size	# Queries	# Templates	# Synthetic Queries	Avg. # Plan Nodes	Maximum Runtime (mins)
TPC-H	SF = 10	570	19	0	14	20
TPC-DS	SF = 1	2700	90	0	29	45
JOB	13GB	3390	113	0	24	60
TPC-H+	SF = 10	950	19	380	10	30
TPC-DS+	SF = 1	4500	90	1800	19	60
JOB+	13GB	5650	113	2260	16	75

can be mitigated by increasing the diversity of encoded information and designing a more effective feature extraction module. U5 is an aleatoric uncertainty that cannot be eliminated due to the inherent randomness of query execution. However, in practice, if the same query is executed multiple times, the average execution time can be used as the estimation target. (2) The uncertainties affecting \mathcal{U}_1 , namely U3 and U4, cannot be completely resolved. It is difficult for the system to gather all possible combinations of queries and index configurations, and the model cannot achieve perfect accuracy on the training data. Consequently, the trained model will inevitably encounter workloads that deviate from those seen during training.

Therefore, when the feature extraction module is effective and the encoded information is sufficient, \mathcal{U}_2 quantification can be disabled. While this may slightly reduce the accuracy of the UQ, it significantly improves the inference efficiency of the BE-UQ model.

5 EMPIRICAL STUDY ON UNCERTAINTY QUANTIFICATION

In this section, we compare different UQ methods from three aspects, namely the UQ capability, the efficiency and the impact on the accuracy of BE.

5.1 Datasets Construction

Three famous database benchmarks are adopted in the empirical study. Table 2 summarizes the databases and the workloads.

TPC-H: Following Leis et al. [38], [39], we randomly generated 30 queries from each template in TPC-H, excluding templates 2, 17, and 20. These were excluded because their queries have significantly longer execution times, which would disproportionately affect the overall workload cost. Indexes accelerating these queries are typically preferred over those for other templates.

TPC-DS: We also randomly generated 30 queries from each template in TPC-DS. Templates 4, 6, 9, 10, 11, 32, 35, 41, and 95 were excluded for the same reason given above.

JOB: This workload consists of 30 queries randomly generated from each template in JOB.

To increase the complexity of index tuning, we ingested synthetic queries into these workloads using the method devised by Yu et al. [39]. The enhanced workloads are referred to as **TPC-H+**, **TPC-DS+** and **JOB+**, respectively.

To the best of our knowledge, no systematic experiments have previously explored uncertainty involved in index tuning tasks. To investigate the impacts of UQ on the accuracy and the efficiency of learning-based benefit estimators, as well as their ability to quantify uncertainty, we designed the following experimental methodology:

We ran the Autoadmin and Extend algorithms on three distinct workloads: **TPC-H+**, **TPC-DS+**, and **JOB+**, under

various budget constraints to collect index configurations for tuning. After materializing these configurations, we gathered query execution data, represented as [(query, index config) \rightarrow benefit], and formed a comprehensive dataset. This dataset was then divided into three segments based on query templates and indexes:

Training Dataset: Used for model training, containing approximately 50% of the total data. This subset only includes some of the query templates and indexes.

Test Dataset: Comprises about 15% of the total data, where each query or index configuration appeared in the training set but was not simultaneously seen by the model. This segment tests the model’s generalization capability within in-domain data.

Uncertainty Dataset: This dataset accounts for about 35% of the total data. It includes queries and indexes that are not present in the first two datasets, and no similar queries (from the same template) appear. For each model mentioned in Subsubsection 5.2.2, we will test using these samples, excluding those with errors below the 90th percentile of the Training Dataset errors. This way, the remaining samples are those the model fails to predict correctly due to U1-U4, and the model should assign a high uncertainty value to them. These samples are designated as **Uncertainty Samples**.

There are two points to note. First, the samples that different models fail to predict accurately vary, resulting in an inconsistent number of **Uncertainty Samples**, but the difference does not exceed 10%. Second, we use query costs to calculate the benefit rather than the execution time of the query, so we do not include U5-type uncertainty samples here.

5.2 Experimental Setup

5.2.1 BE Models

In this experiment, we adopt two well-known learning-based BE models:

(1) **LIB.** The BE model proposed in [7] encodes the operators and information in a query plan that can be influenced by indexes, forming a variable-length Index Optimizable Operations Set. After encoding through Multi-head Attention, the pooling operation retrieves v^h , culminating in the output of the BE via a MLP.

(2) **AMA.** The model in [6] utilizes multiple channels to extract information and employs a weighted sum to compare query plans, selecting the faster option. Following [7], we replaced AMA’s classification layer with an MLP for benefit estimation.

It is important to note that while we aim to maintain consistency with the original paper regarding the two BE models, complete consistency may not be achievable. Our primary focus is on studying the impact of the UQ method rather than directly comparing the two BE models.

5.2.2 UQ Methods

We integrate five types of UQ methods into the aforementioned BE models, forming sixteen distinct BE-UQ models for our experiment:

(1) **Ours.** This model integrates the hybrid quantification method proposed in this paper, resulting in LIB-Hybrid and AMA-Hybrid. We also compare an alternative version that utilizes efficiency enhancements, represented as LIB-AE and AMA-AE.

(2) **BNN**. We replace the MLP in the Prediction Module of both models with BNN, forming LIB-BNN and AMA-BNN.

(3) **MCD**. We compare three variants of this method in the experiment [40]: the first variant replaces all dropout layers in the model with MCD, resulting in LIB-MCD-all and AMA-MCD-all. The second variant applies MCD only to the last layer of the model’s Prediction Module, forming LIB-MCD-last and AMA-MCD-last. The third variant adopts the approach proposed in [37], which utilizes determinantal point processes for sampling to enhance diversity with minimal inference time increase, forming LIB-MCD-dpp and AMA-MCD-dpp.

In addition to the above methods, we also compare two other types of UQ methods.

(4) **Ensemble**. Ensemble methods refer to machine learning techniques such as Bagging and Boosting, which create multiple models and then combine them to produce improved predictions. Ensemble methods generally yield more accurate results than any single model. Lakshminarayanan et al. [32] utilize ensemble methods to quantify model uncertainty. A set of models can be induced either independently (e.g., in Bagging) or dependently (e.g., in Boosting). Given a test record \mathbf{x} as input, these models produce outputs $\hat{y}_1, \hat{y}_2, \dots, \hat{y}_m$, respectively. The mean of $\hat{y}_1, \hat{y}_2, \dots, \hat{y}_m$ serves as the prediction for \mathbf{x} , while the variance of $\hat{y}_1, \hat{y}_2, \dots, \hat{y}_m$ indicates the uncertainty of the ensemble model regarding \mathbf{x} .

During hyperparameter selection, we retain the five best performing models for LIB and AMA, creating the LIB-Ensemble and AMA-Ensemble.

(5) **HSTO**. [30] proposed Hierarchical Stochastic Self-Attention (HSTO) to replace the existing Self-Attention mechanism, enabling all models using Self-Attention to quantify uncertainty. This method utilizes the Gumbel-Softmax to transform the deterministic attention distribution for values in each attention head into a stochastic one. The prediction and uncertainty for a given test record \mathbf{x} are obtained similarly to the MCD method.

Since this method relies on the Self-Attention module within the model, it is applicable only to LIB. We adopt the two versions mentioned in the original paper, resulting in LIB-STO and LIB-HSTO.

5.2.3 Implementation

We set the relative benefit $rb = \frac{B(q, \mathcal{I}_0, \mathcal{I})}{c(q, \mathcal{I}_0)}$ as the prediction target. To maintain compatibility with the LIB framework, we exclude data entries that exhibit negative benefits from our dataset. For each model discussed, we generate thirty sets of hyperparameters and train on the training dataset. Subsequently, we retain the model that demonstrates the best performance based on evaluations using the test dataset.

When quantifying uncertainty, we use the variance of results from five models as the quantification of uncertainty for the ensemble-based model. For other models, we perform inference 20 times [37] for each batch sample, using variance as the quantification of uncertainty.

5.2.4 Hardware & Software

The experiments were carried out on a Ubuntu server with two Intel Xeon 4210R CPUs (10 cores, 2.40GHz), 256GB of

TABLE 3: Percentage of Uncertainty Samples exceeding the uncertainty threshold set by the Training Dataset.

LIB-based Model	TPC-H+	TPC-DS+	JOB+	AMA-based Model	TPC-H+	TPC-DS+	JOB+
BNN	13.03	40.20	16.04	BNN	45.26	65.32	53.67
MCD-all	68.08	40.98	26.22	MCD-all	51.73	54.17	45.61
MCD-last	61.79	29.32	5.92	MCD-last	21.76	21.27	22.11
MCD-dpp	16.02	36.91	8.35	MCD-dpp	78.28	34.83	30.76
Ensemble	79.01	53.44	29.32	Ensemble	38.73	77.62	60.22
AE	71.85	31.13	30.93	AE	92.68	84.19	61.00
Hybrid	81.80	57.65	32.88	Hybrid	91.74	78.13	47.82
\mathcal{U}_1	51.88	27.21	20.68	\mathcal{U}_1	88.87	54.21	20.00
\mathcal{U}_2	59.70	43.46	20.76	\mathcal{U}_2	54.93	47.50	34.87
STO	68.41	34.86	23.51				
HSTO	63.64	35.13	24.58				

main memory, and one NVIDIA GeForce RTX 3060 GPU. The DBMS is PostgreSQL 12.13.

5.3 Results on Uncertainty Quantification

We present Raincloud plots illustrating the uncertainty distributions for sixteen models across various benchmarks. Figure 8 displays the plots for models based on BNN, MCD, Ensemble, and HSTO. Figures 9 and 10 show the plots for models based on Hybrid and AE, respectively. Each subplot depicts the uncertainty distribution of samples as calculated by the model for the training dataset, test dataset, and Uncertainty Samples. Consequently, the greater the uncertainty of the orange samples representing Uncertainty Samples in the graph and the higher their differentiation from other samples, the more precisely the model’s uncertainty modeling is demonstrated, enabling it to effectively distinguish uncertainty data. The red lines in the graphs represent the average uncertainties across the three datasets.

Table 3 further illustrates the filtering capabilities of various methods for Uncertainty Samples. Since Hybrid includes two UQ modules, we adopt the following approach to ensure comparability with other models: for \mathcal{U}_1 and \mathcal{U}_2 , we select the 90th percentile of the uncertainty distribution from the Training Dataset as their corresponding thresholds. We calculate the proportion P of samples in the Training Dataset with uncertainty values lower than these thresholds. If \mathcal{U}_1 and \mathcal{U}_2 are probabilistically independent, this proportion should be 81%. For other models with only one UQ module, we employ the P -th percentile of the uncertainty distribution from the Training Dataset as a threshold. The table shows the proportion of samples in the Uncertainty Samples that exceed this threshold. The higher the proportion, the stronger the model’s ability to identify uncertain samples. For each benchmark in the table, we highlight the model with the most effective filtering in green and the second most effective in blue. Note that \mathcal{U}_1 and \mathcal{U}_2 , as parts of the Hybrid, are excluded from this ranking.

From these results, we can draw the following conclusions:

First, the AE and Hybrid models consistently perform the best, followed by the Ensemble method. The other methods lag significantly behind in both stability and optimal performance in UQ. The best performance is seen with the AMA-AE model under the TPC-H+, which can identify 92.68% of Uncertainty Samples while misclassifying about 19% of training samples, significantly outperforming general-purpose methods. In more than two-thirds of the benchmarks, the AE and Hybrid models consistently rank among the top two, demonstrating better stability than the Ensemble method.

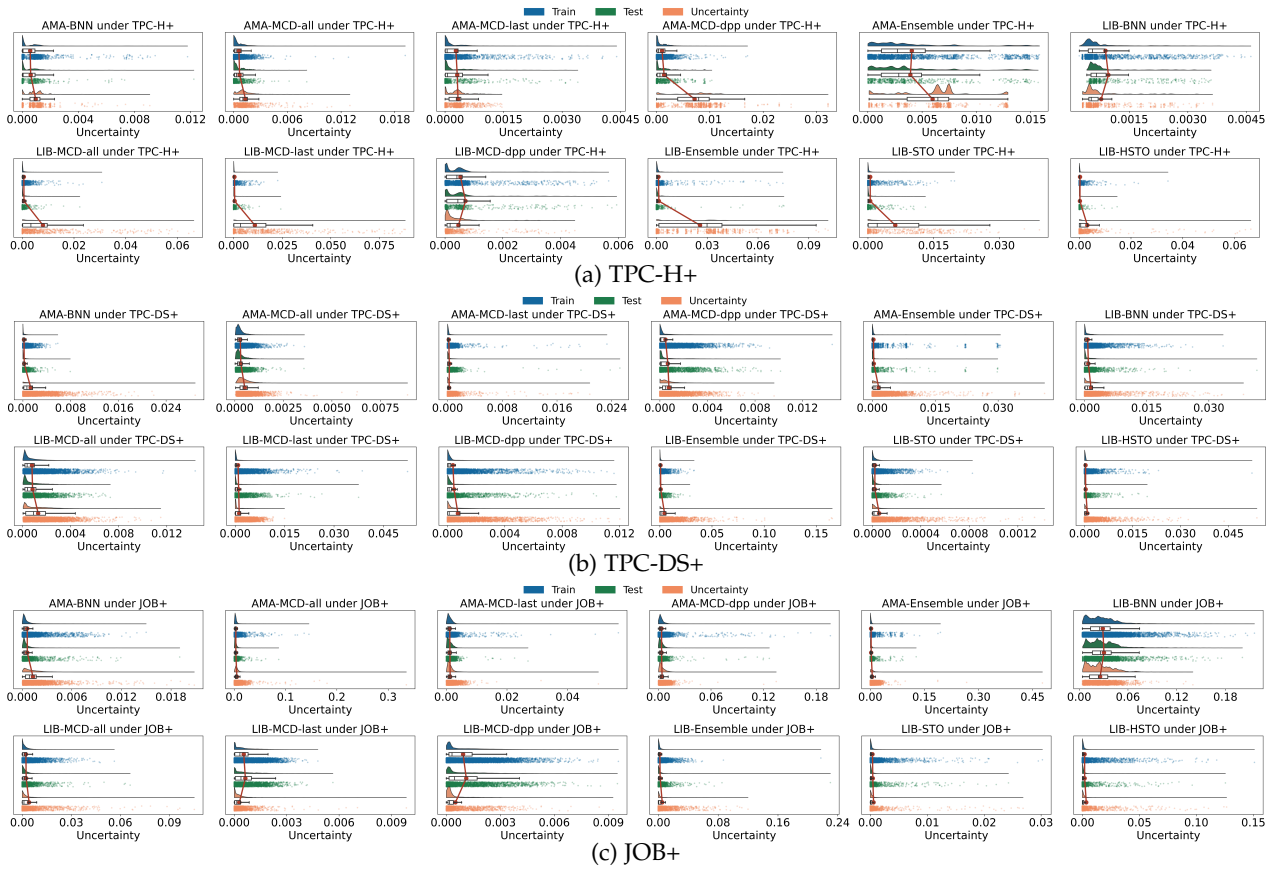


Fig. 8: Uncertainty distribution of models using BNN, MCD, Ensemble, and HSTO.

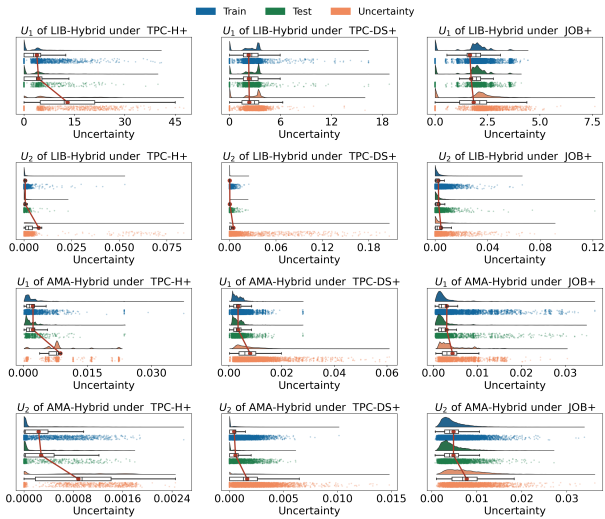


Fig. 9: Uncertainty distribution of models using Hybrid.

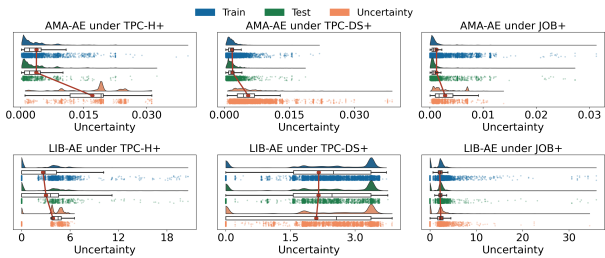


Fig. 10: Uncertainty distribution of models using AE.

Second, the quality of uncertainty quantification is related to the base model and dataset. Across three bench-

marks, the uncertainty modeling quality of the AMA base model consistently surpasses that of the LIB model, particularly evident in the proposed AE and Hybrid models. This may be attributed to the fact that the model’s ability to fit the data also determines its accuracy and capability in UQ. As illustrated in Table 5, AMA’s accuracy is significantly higher than LIB’s. Accurate results necessitate effective encoding of inputs into a hidden vector, the foundational principle of our methodology, which accounts for these observations.

Overall, these 16 models demonstrate superior performance on the TPC-H+ benchmark compared to TPC-DS+, with the poorest performance observed on the JOB+ benchmark, where the most effective UQ methods filter only 61% of Uncertainty Samples.

Third, the settings for uncertainty thresholds significantly impact the ability to detect Uncertainty Samples. Uncertainty distribution within a dataset is usually confined to a narrow range, and the relationship between the threshold and this range dictates the model’s detection capabilities. For example, in the AMA-Ensemble model under TPC-H+, setting a filtering threshold at the 81th percentile of the training dataset excludes only 38.73% of Uncertainty Samples, whereas a threshold at the 75th percentile increases exclusion to 73.34%.

Fourth, HSTO, specifically designed for Self-Attention, did not demonstrate improved performance on this task. Neither model achieved optimal performance across the three benchmarks.

Fifth, among the three MCD-based methods, MCD-all outperforms the others, achieving optimal results in five out of six scenarios. MCD-dpp provides a richer sampling diversity compared to MCD-last and outperforms it in the

TABLE 4: Time for model inference per batch (ms).

Model	TPC-H+	TPC-DS+	JOB+	Model	TPC-H+	TPC-DS+	JOB+
LIB	2.76	2.30	5.58	AMA	0.18	0.18	0.25
BNN	61.85	44.46	50.75	BNN	10.77	7.41	10.54
MCD-all	184.59	45.03	155.14	MCD-all	6.19	2.94	4.90
MCD-last	60.00	89.63	133.04	MCD-last	5.23	4.13	5.23
MCD-dpp	60.01	147.86	83.63	MCD-dpp	260.82	78.39	51.45
Ensemble	22.72	14.15	29.90	Ensemble	1.82	0.80	1.71
AE	3.08	4.76	6.37	AE	0.52	0.51	0.51
Hybrid	60.74	103.95	98.16	Hybrid	10.28	9.82	9.26
STO	151.40	137.33	157.01				
HSTO	64.46	109.25	327.03				

majority of scenarios.

5.4 Results on Prediction Accuracy and Inference Efficiency

Table 4 shows the time taken by different models to process a single batch, which includes predicting the relative error $\hat{r}b_{predicted}$ and estimating uncertainty, in milliseconds. Models in which the inference time with UQ is on the same order of magnitude as the base model are marked in green.

The primary factors influencing inference efficiency are the base model structure, model hyperparameters, and methods for UQ. LIB, utilizing heavier Multi-head Attention, requires significantly more inference time, up to an order of magnitude higher than AMA. For the models based on the same BE model, the optimal hyperparameters vary across different datasets, which can also lead to several times difference in inference efficiency. Methods like BNN, MCD, and HSTO necessitate multiple inferences on the same model, resulting in inference times that are proportionally related to the number of inferences, significantly exceeding the base model and AE by one to two orders of magnitude. Specifically, MCD-dpp introduces extra computational overhead due to sampling processes, notably affecting the faster base model AMA, and to a lesser extent, the heavier LIB model where it is less of a determining efficiency factor. The inference time for Ensemble models scales with the number of models involved; selecting five models during hyperparameter tuning has resulted in higher overall efficiency compared to other multiple-inference UQ methods. Of all methods evaluated, AE proves the most efficient, necessitating only an additional inference for the decoder network, which keeps its inference times close to those of the base model on all six benchmarks.

Table 5 evaluates the impact of incorporating UQ methods into BE models. We assess performance using the absolute difference between predicted and actual values, i.e. $|rb_{actual} - \hat{r}b_{predicted}|$. The table shows the 50th, 95th, and 99th percentiles of error distributions for LIB and AMA. For models to which UQ methods have been added, the table shows the change in error relative to the base model, where models that have the most negative impact are marked in red, and those with the most positive impact are marked in green.

Among all UQ methods, only BNN significantly affected the accuracy of the BE model, while the other methods had no substantial impact. Each model was retrained using 30 distinct sets of hyperparameters, so any minor variations in accuracy can be attributed to differences in hyperparameter settings. In the case of BNN, however, each neuron is replaced by a value sampled from a distribution, which effectively doubles the number of network parameters (as each deterministic neuron corresponds to values such as

mean, variance, etc., in BNN) and significantly expands the hyperparameter space (e.g., requiring a prior distribution). This makes the training process fundamentally different and more complex, requiring more intensive hyperparameter tuning.

Comparing to the MCD-last, MCD-dpp had a higher effect on accuracy when AMA was used as the base model, more inference burden while more UQ capability, making it better suited for integration with heavier base models, which might be related to the changes it made in the sampling process during inference. However, more research is needed to provide a definitive conclusion, which is beyond the scope of this study.

Among the other methods, since the AE method did not alter the original structure and parameters of the BE model after training, it theoretically should not affect the accuracy of the BE model.

6 EMPIRICAL STUDY ON INDEX TUNING

6.1 Experimental Setup

In this section, we explore whether modeling uncertainty can enhance index tuning results. Therefore, we integrated the aforementioned BE model into the BEAUTY framework and performed index tuning on six benchmarks under different budget constraints.

6.1.1 Implementation

Leis et al. [38] show that no single index configuration enumeration algorithm delivers optimal performance in all scenarios. In our experiments, we used DTA [14], which balances runtime and solution quality well across various scenarios. This algorithm has a set maximum runtime and stops after enumerating all configurations or reaching this limit. However, following Leis et al.’s [38] implementation, the algorithm completes the current seed’s configuration even if it exceeds the time limit, occasionally surpassing the maximum runtime. We adjust the maximum runtime based on workload size, as shown in Table 2.

Based on the performance of various models mentioned in Section 5, we selected nine models in our experiment: LIB, LIB-Ensemble, LIB-AE, LIB-Hybrid, AMA, AMA-Ensemble, AMA-AE, AMA-Hybrid, and what-if. The thresholds for each model were set as described in Subsection 5.3. When the uncertainty value of the benefits estimated by the BE-UQ model for a sample exceeds the threshold, we use what-if tools to estimate the benefits of that sample.

6.1.2 Evaluation Metrics

We use specific metrics to assess the performance of index tuning. Given a workload W , \mathcal{I}_0 represents the initial set of indexes, and \mathcal{I} the set of selected indexes. We measure the quality of replacing \mathcal{I}_0 with \mathcal{I} by the relative improvement in W ’s cost: $\max\left(0, \frac{B(W, \mathcal{I}_0, \mathcal{I})}{c(W, \mathcal{I}_0)}\right) = \max\left(0, 1 - \frac{c(W, \mathcal{I})}{c(W, \mathcal{I}_0)}\right)$.

On some occasions, if the selected indexes increase the cost, they must be discarded, and thus the improvement in cost is zero.

6.2 Results on Index Tuning

Figure 11 illustrates the index tuning results of nine methods under various budgets across six benchmarks. Table 6

TABLE 5: The impact of uncertainty quantification methods on the prediction errors. Models that have the most negative impact are marked in red, while those with the most positive impact are marked in green.

Dataset		LIB	BNN	MCD-all	MCD-last	MCD-dpp	Ensemble	STO	HSTO	AE	Hybrid	AMA	BNN	MCD-all	MCD-last	MCD-dpp	Ensemble	AE	Hybrid
TPC-H+	50th	0.13	+0.10	+0.01	+0.02	+0.04	+0.00	+0.03	+0.00	+0.09	+0.05	0.01	+0.02	+0.00	+0.00	+0.02	+0.02	+0.00	+0.00
	95th	0.47	+0.02	+0.00	+0.00	-0.04	+0.00	+0.00	+0.00	+0.05	+0.01	0.05	+0.06	+0.01	+0.03	+0.00	+0.03	+0.00	+0.02
	99th	0.65	-0.11	-0.05	-0.04	-0.07	-0.01	+0.00	-0.05	-0.12	-0.01	0.11	+0.07	+0.00	+0.00	+0.03	+0.01	-0.03	+0.02
TPC-DS+	50th	0.06	+0.01	+0.00	-0.01	+0.00	+0.00	+0.00	+0.00	+0.00	+0.00	0.01	+0.01	+0.00	+0.00	+0.00	+0.00	+0.00	+0.00
	95th	0.44	+0.03	+0.00	-0.02	+0.01	+0.00	+0.00	+0.00	+0.00	+0.00	0.20	+0.06	+0.02	+0.00	+0.09	+0.03	+0.01	+0.01
	99th	0.71	+0.00	+0.00	+0.03	+0.00	+0.00	+0.00	+0.00	+0.02	+0.00	0.34	+0.08	+0.06	+0.05	+0.07	+0.04	+0.05	+0.07
JOB+	50th	0.19	+0.13	+0.01	+0.03	+0.04	+0.00	+0.04	+0.05	+0.03	+0.01	0.03	+0.02	+0.00	+0.00	+0.05	+0.00	+0.00	+0.01
	95th	0.57	+0.04	+0.00	+0.00	+0.00	+0.00	+0.02	+0.00	+0.03	+0.00	0.19	+0.06	-0.01	+0.00	+0.05	+0.00	+0.00	+0.04
	99th	0.76	+0.16	-0.02	+0.02	+0.00	-0.02	+0.07	+0.09	+0.04	+0.04	0.37	+0.17	+0.00	+0.00	+0.11	+0.00	+0.08	+0.10

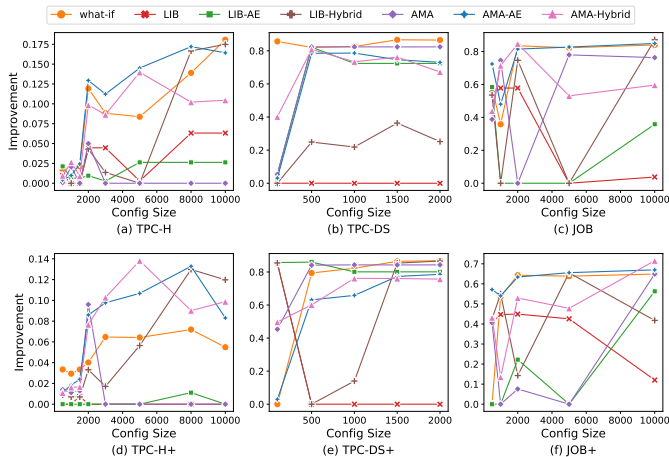


Fig. 11: Cost improvements achieved by different benefit estimation models.

TABLE 6: Rankings of cost improvements achieved by models.

Method	# 1st Place	# 2nd Place	# 3rd Place	# Worst
What-if	8	8	11	1
LIB	0	0	1	10
LIB-Ensemble	1	4	4	3
LIB-AE	3	1	1	4
LIB-Hybrid	3	7	0	4
AMA	3	3	3	6
AMA-Ensemble	4	2	6	7
AMA-AE	10	7	5	0
AMA-Hybrid	4	4	5	0

presents detailed statistics of cost improvements, highlighting the best performances in green and the second best in blue. From these results, we can draw the following conclusions:

First, integrating the UQ module into the two base models significantly improved index tuning results. The LIB model has seen a significant reduction in the number of worst-case scenarios, while the AMA model has experienced a substantial increase in the number of optimal configurations. Additionally, when integrating AE and Hybrid into the AMA model, the number of worst-case scenarios decreased from six to zero.

Second, the performance of the integrated Hybrid model is superior to that of the Ensemble-based model. As shown in Table 3, Hybrid’s ability to quantify uncertainty surpasses that of Ensemble, allowing it to more accurately identify the parts of the learning-based BE model that it cannot accurately estimate, thereby improving BE’s accuracy. The DTA algorithm requires a specified maximum runtime, and usually, it cannot enumerate all index configurations by the end. Therefore, the greater the delay in BE-UQ inference, the fewer configurations the index advisor can explore. As seen in Table 4, Hybrid has a higher delay. Thus, by provid-

ing more accurate uncertainty quantifications, Hybrid finds better results with fewer configurations.

Third, AE’s results are slightly better than Hybrid’s. The accuracy of the LIB base model is not high, and in this situation, Hybrid’s UQ accuracy is higher than AE’s, enabling it to identify as many uncertain data points as possible, resulting in better performance than AE. Conversely, when using AMA as the base model, AE achieves higher identification accuracy and lower inference delay, allowing for more accurate enumeration of more index configurations. Therefore, it achieves the highest number of optimal configurations and surpasses the what-if tools. For index tuning tasks, Hybrid is preferable when there is sufficient time available for tuning. If time is limited and the BE model demonstrates high accuracy, selecting AE can result in a better index configuration.

Fourth, in scenarios abundant with Uncertainty Samples, the what-if approach remains a stable and precise method, achieving the best or nearly the best results across all six benchmarks. This consistency forms the foundation of our study, which aims to model the uncertainty in learning-based models, combining their accuracy and efficiency with the reliability of what-if tools.

7 RELATED WORK

We presented the related work on UQ in subsection 2.3 and subsection 5.2. The related work on learning-based BE models is detailed in subsection 2.2. In this section, we introduce additional related work on index tuning.

Index Configuration Enumeration. Early greedy enumeration algorithms typically follow two strategies [38]. One is a top-down approach [21], such as the Drop algorithm [13], which iteratively removes candidate indexes with minimal impact on workload execution time until the budget constraint is met. The other is a bottom-up approach [14], exemplified by the Autoadmin algorithm proposed by Chaudhuri and Narasayya [12], which starts with an empty set and adds indexes until the maximum budget is reached. Recently, reinforcement learning-based methods, such as those by Lan et al. [11] and Sadri et al. [41], have shown greater adaptability and efficiency. SmartIX [42] introduces add/delete operations based on environmental state.

Workload Compression. To enhance the efficiency of index tuning, many approaches perform workload compression prior to tuning. Sadri et al. [41] identify templates based on the non-parameterized portions of query statements, retaining one query for each template. However, the query plans of a template can vary greatly depending on parameter differences, resulting in substantially different benefits calculated for the same index configuration and causing significant workload information loss. Furthermore,

RIBE [39] clusters queries based on operators within the query plan, ensuring that only redundant information from the workload is eliminated. Besides these clustering-based methods, GSUM [2] and ISUM [43] define various query features and design greedy algorithms that flexibly determine the number of queries in the workload.

8 CONCLUSION

In this paper, we address a critical yet unexplored question: Can uncertainty enable better learning-based index tuning? To answer this question, we focus on the core component of index tuning, prioritizing improvements to the learning-based BE model. Our investigation is divided into two sub-questions: (1) Can UQ methods accurately measure the reliability of model results? (2) How can a BE model that provides uncertainty estimates be integrated into an index advisor, and what are the implications of this integration?

To address these two questions, we first analyze the origins and characteristics of model uncertainty in BE tasks. Unlike existing general UQ methods, we design a new hybrid quantification framework tailored to the task's characteristics and propose an alternative version to enhance efficiency. Experimental validation shows that our method outperforms existing quantification methods in five out of six scenarios. The alternative version significantly improves UQ efficiency, albeit with a slight reduction in quantification accuracy. Next, we verified that the BEAUTY framework leverages the stability of what-if tools to supplement the learning-based BE model. In end-to-end experiments, this framework significantly improves the quality of index tuning results.

Our findings confirm that integrating uncertainty can enhance learning-based index tuning. Our framework focuses on the BE problem, marking an initial exploration in this area. Future research will investigate the role of uncertainty in other index advisor modules.

ACKNOWLEDGMENTS

This work was partially supported by the National Natural Science Foundation of China (Grant No. 62072138).

REFERENCES

- [1] T. Siddiqui, W. Wu, V. Narasayya, and S. Chaudhuri, "Distill: Low-overhead data-driven techniques for filtering and costing indexes for scalable index tuning," *Proc. VLDB Endow.*, vol. 15, no. 10, pp. 2019–2031, 2022.
- [2] S. Deep, A. Gruenheid, P. Koutris, J. Naughton, and S. Vlas, "Comprehensive and efficient workload compression," *Proc. VLDB Endow.*, vol. 14, no. 3, pp. 418–430, 2020.
- [3] S. Chaudhuri and V. Narasayya, "Autoadmin "what-if" index analysis utility," *SIGMOD Rec.*, vol. 27, no. 2, p. 367–378, jun 1998.
- [4] W. Wu, C. Wang, T. Siddiqui, J. Wang, V. R. Narasayya, S. Chaudhuri, and P. A. Bernstein, "Budget-aware index tuning with reinforcement learning," in *SIGMOD '22: International Conference on Management of Data, Philadelphia, PA, USA, June 12 - 17, 2022*, Z. G. Ives, A. Bonifati, and A. E. Abbadi, Eds. ACM, 2022, pp. 1528–1541. [Online]. Available: <https://doi.org/10.1145/3514221.3526128>
- [5] Z. Wang, Q. Zeng, N. Wang, H. Lu, and Y. Zhang, "CEDA: learned cardinality estimation with domain adaptation," *Proc. VLDB Endow.*, vol. 16, no. 12, pp. 3934–3937, 2023. [Online]. Available: <https://www.vldb.org/pvldb/vol16/p3934-wang.pdf>
- [6] B. Ding, S. Das, R. Marcus, W. Wu, S. Chaudhuri, and V. R. Narasayya, "AI meets AI: leveraging query executions to improve index recommendations," in *Proceedings of the 2019 International Conference on Management of Data, SIGMOD Conference 2019, Amsterdam, The Netherlands, June 30 - July 5, 2019*, P. A. Boncz, S. Manegold, A. Ailamaki, A. Deshpande, and T. Kraska, Eds. ACM, 2019, pp. 1241–1258. [Online]. Available: <https://doi.org/10.1145/3299869.3324957>
- [7] J. Shi, G. Cong, and X. Li, "Learned index benefits: Machine learning based index performance estimation," *Proc. VLDB Endow.*, vol. 15, no. 13, pp. 3950–3962, 2022. [Online]. Available: <https://www.vldb.org/pvldb/vol15/p3950-shi.pdf>
- [8] T. Nair, D. Precup, D. L. Arnold, and T. Arbel, "Exploring uncertainty measures in deep networks for multiple sclerosis lesion detection and segmentation," *Medical Image Anal.*, vol. 59, 2020. [Online]. Available: <https://doi.org/10.1016/j.media.2019.101557>
- [9] D. Feng, L. Rosenbaum, and K. Dietmayer, "Towards safe autonomous driving: Capture uncertainty in the deep neural network for lidar 3d vehicle detection," in *21st International Conference on Intelligent Transportation Systems, ITSC 2018, Maui, HI, USA, November 4-7, 2018*, W. Zhang, A. M. Bayen, J. J. S. Medina, and M. J. Barth, Eds. IEEE, 2018, pp. 3266–3273. [Online]. Available: <https://doi.org/10.1109/ITSC.2018.8569814>
- [10] Y. Zhang and A. A. Lee, "Bayesian semi-supervised learning for uncertainty-calibrated prediction of molecular properties and active learning," *CoRR*, vol. abs/1902.00925, 2019. [Online]. Available: <http://arxiv.org/abs/1902.00925>
- [11] H. Lan, Z. Bao, and Y. Peng, "An index advisor using deep reinforcement learning," in *CIKM '20: The 29th ACM International Conference on Information and Knowledge Management, Virtual Event, Ireland, October 19-23, 2020*, M. d'Aquin, S. Dietze, C. Hauff, E. Curry, and P. Cudré-Mauroux, Eds. ACM, 2020, pp. 2105–2108. [Online]. Available: <https://doi.org/10.1145/3340531.3412106>
- [12] S. Chaudhuri and V. R. Narasayya, "An efficient cost-driven index selection tool for microsoft SQL server," in *VLDB'97, Proceedings of 23rd International Conference on Very Large Data Bases, August 25-29, 1997, Athens, Greece*, M. Jarke, M. J. Carey, K. R. Dittrich, F. H. Lochovsky, P. Loucopoulos, and M. A. Jeusfeld, Eds. Morgan Kaufmann, 1997, pp. 146–155.
- [13] K.-Y. Whang, "Index selection in relational databases," in *Foundations of Data Organization*. Springer, 1987, pp. 487–500.
- [14] S. Chaudhuri and V. Narasayya, "Anytime algorithm of database tuning advisor for microsoft sql server," <https://www.microsoft.com/en-us/research/publication/anytime-algorithm-of-database-tuning-advisor-for-microsoft-sql-server/>, June 2020, visited 2024-10-16.
- [15] D. Dash, N. Polyzotis, and A. Ailamaki, "Cophy: A scalable, portable, and interactive index advisor for large workloads," *Proc. VLDB Endow.*, vol. 4, no. 6, pp. 362–372, 2011. [Online]. Available: <http://www.vldb.org/pvldb/vol4/p362-dash.pdf>
- [16] R. M. Perera, B. Oetomo, B. I. P. Rubinstein, and R. Borovica-Gajic, "No dba? no regret! multi-armed bandits for index tuning of analytical and htap workloads with provable guarantees," *IEEE Transactions on Knowledge and Data Engineering*, vol. 35, no. 12, pp. 12 855–12 872, 2023.
- [17] R. M. Perera, B. Oetomo, B. I. P. Rubinstein, and R. Borovica-Gajic, "HMAB: self-driving hierarchy of bandits for integrated physical database design tuning," *Proc. VLDB Endow.*, vol. 16, no. 2, pp. 216–229, 2022. [Online]. Available: <https://www.vldb.org/pvldb/vol16/p216-perera.pdf>
- [18] J. Kossmann, A. Kastius, and R. Schlosser, "SWIRL: selection of workload-aware indexes using reinforcement learning," in *Proceedings of the 25th International Conference on Extending Database Technology, EDBT 2022, Edinburgh, UK, March 29 - April 1, 2022*, J. Stoyanovich, J. Teubner, P. Guagliardo, M. Nikolic, A. Pieris, J. Mühlhig, F. Özcan, S. Schelter, H. V. Jagadish, and M. Zhang, Eds. OpenProceedings.org, 2022, pp. 2:155–2:168. [Online]. Available: <https://doi.org/10.48786/edbt.2022.06>
- [19] V. Sharma and C. Dyreson, "Indexer++: Workload-aware online index tuning with transformers and reinforcement learning," in *Proceedings of the 37th ACM/SIGAPP Symposium on Applied Computing, ser. SAC '22*. Association for Computing Machinery, 2022, pp. 372–380.
- [20] R. Schlosser, J. Kossmann, and M. Boissier, "Efficient scalable multi-attribute index selection using recursive strategies," in *2019 IEEE 35th International Conference on Data Engineering (ICDE)*. IEEE, 2019, pp. 1238–1249.
- [21] N. Bruno and S. Chaudhuri, "Automatic physical database tuning: A relaxation-based approach," in *Proceedings of the ACM SIGMOD*

- International Conference on Management of Data, Baltimore, Maryland, USA, June 14-16, 2005*, F. Özcan, Ed. ACM, 2005, pp. 227–238. [Online]. Available: <https://doi.org/10.1145/1066157.1066184>
- [22] J. Gawlikowski, C. R. N. Tassi, M. Ali, J. Lee, M. Humt, J. Feng, A. M. Kruspe, R. Triebel, P. Jung, R. Roscher, M. Shahzad, W. Yang, R. Bamler, and X. Zhu, “A survey of uncertainty in deep neural networks,” *Artif. Intell. Rev.*, vol. 56, no. S1, pp. 1513–1589, 2023. [Online]. Available: <https://doi.org/10.1007/s10462-023-10562-9>
- [23] E. Hüllermeier and W. Waegeman, “Aleatoric and epistemic uncertainty in machine learning: an introduction to concepts and methods,” *Mach. Learn.*, vol. 110, no. 3, pp. 457–506, 2021. [Online]. Available: <https://doi.org/10.1007/s10994-021-05946-3>
- [24] M. Abdar, F. Pourpanah, S. Hussain, D. Rezaadegan, L. Liu, M. Ghavamzadeh, P. W. Fieguth, X. Cao, A. Khosravi, U. R. Acharya, V. Makarencov, and S. Nahavandi, “A review of uncertainty quantification in deep learning: Techniques, applications and challenges,” *Inf. Fusion*, vol. 76, pp. 243–297, 2021. [Online]. Available: <https://doi.org/10.1016/j.inffus.2021.05.008>
- [25] J. S. Denker, D. B. Schwartz, B. S. Wittner, S. A. Solla, R. E. Howard, L. D. Jackel, and J. J. Hopfield, “Large automatic learning, rule extraction, and generalization,” *Complex Syst.*, vol. 1, no. 5, 1987. [Online]. Available: http://www.complex-systems.com/abstracts/v01_i05_a02.html
- [26] M. Oppner and C. Archambeau, “The variational gaussian approximation revisited,” *Neural Comput.*, vol. 21, no. 3, pp. 786–792, 2009. [Online]. Available: <https://doi.org/10.1162/neco.2008.08-07-592>
- [27] Y. Gal and Z. Ghahramani, “Dropout as a bayesian approximation: Representing model uncertainty in deep learning,” in *Proceedings of the 33rd International Conference on Machine Learning, ICML 2016, New York City, NY, USA, June 19-24, 2016*, ser. JMLR Workshop and Conference Proceedings, M. Balcan and K. Q. Weinberger, Eds., vol. 48. JMLR.org, 2016, pp. 1050–1059. [Online]. Available: <http://proceedings.mlr.press/v48/gal16.html>
- [28] L. K. Hansen and P. Salamon, “Neural network ensembles,” *IEEE Trans. Pattern Anal. Mach. Intell.*, vol. 12, no. 10, pp. 993–1001, 1990. [Online]. Available: <https://doi.org/10.1109/34.58871>
- [29] G. D. C. Cavalcanti, L. S. Oliveira, T. J. M. Moura, and G. V. Carvalho, “Combining diversity measures for ensemble pruning,” *Pattern Recognit. Lett.*, vol. 74, pp. 38–45, 2016. [Online]. Available: <https://doi.org/10.1016/j.patrec.2016.01.029>
- [30] J. Pei, C. Wang, and G. Szarvas, “Transformer uncertainty estimation with hierarchical stochastic attention,” in *Thirty-Sixth AAAI Conference on Artificial Intelligence, AAAI 2022, Thirty-Fourth Conference on Innovative Applications of Artificial Intelligence, IAAI 2022, The Twelfth Symposium on Educational Advances in Artificial Intelligence, EAAI 2022 Virtual Event, February 22 - March 1, 2022*. AAAI Press, 2022, pp. 11147–11155. [Online]. Available: <https://doi.org/10.1609/aaai.v36i10.21364>
- [31] C. Blundell, J. Cornebise, K. Kavukcuoglu, and D. Wierstra, “Weight uncertainty in neural networks,” *CoRR*, vol. abs/1505.05424, 2015. [Online]. Available: <http://arxiv.org/abs/1505.05424>
- [32] B. Lakshminarayanan, A. Pritzel, and C. Blundell, “Simple and scalable predictive uncertainty estimation using deep ensembles,” in *Advances in Neural Information Processing Systems 30: Annual Conference on Neural Information Processing Systems 2017, December 4-9, 2017, Long Beach, CA, USA*, I. Guyon, U. von Luxburg, S. Bengio, H. M. Wallach, R. Fergus, S. V. N. Vishwanathan, and R. Garnett, Eds., 2017, pp. 6402–6413. [Online]. Available: <https://proceedings.neurips.cc/paper/2017/hash/9ef2ed4b7fd2c810847ffa5fa85bce38-Abstract.html>
- [33] F. Hutter, H. H. Hoos, and K. Leyton-Brown, “Sequential model-based optimization for general algorithm configuration,” in *Learning and Intelligent Optimization - 5th International Conference, LION 5, Rome, Italy, January 17-21, 2011. Selected Papers*, ser. Lecture Notes in Computer Science, C. A. C. Coello, Ed., vol. 6683. Springer, 2011, pp. 507–523. [Online]. Available: https://doi.org/10.1007/978-3-642-25566-3_40
- [34] M. Lindauer, K. Eggensperger, M. Feurer, A. Biedenkapp, D. Deng, C. Benjamins, T. Ruhkopf, R. Sass, and F. Hutter, “SMAC3: A versatile bayesian optimization package for hyperparameter optimization,” *J. Mach. Learn. Res.*, vol. 23, pp. 54:1–54:9, 2022. [Online]. Available: <http://jmlr.org/papers/v23/21-0888.html>
- [35] G. Dong, G. Liao, H. Liu, and G. Kuang, “A review of the autoencoder and its variants: A comparative perspective from target recognition in synthetic-aperture radar images,” *IEEE Geoscience and Remote Sensing Magazine*, vol. 6, no. 3, pp. 44–68, 2018.
- [36] A. Graves, “Practical variational inference for neural networks,” in *Advances in Neural Information Processing Systems 24: 25th Annual Conference on Neural Information Processing Systems 2011. Proceedings of a meeting held 12-14 December 2011, Granada, Spain*, J. Shawe-Taylor, R. S. Zemel, P. L. Bartlett, F. C. N. Pereira, and K. Q. Weinberger, Eds., 2011, pp. 2348–2356. [Online]. Available: <https://proceedings.neurips.cc/paper/2011/hash/7eb3c8be3d41e8ebfab08eba5f49632-Abstract.html>
- [37] K. Fedyanin, E. Tsymbalov, and M. Panov, “Dropout strikes back: Improved uncertainty estimation via diversity sampling,” in *International Conference on Analysis of Images, Social Networks and Texts*. Springer, 2021, pp. 125–137.
- [38] J. Kossmann, S. Halfpap, M. Jankrift, and R. Schlosser, “Magic mirror in my hand, which is the best in the land?: An experimental evaluation of index selection algorithms,” *Proc. VLDB Endow.*, vol. 13, no. 12, pp. 2382–2395, 2020.
- [39] T. Yu, Z. Zou, W. Sun, and Y. Yan, “Refactoring index tuning process with benefit estimation,” *Proc. VLDB Endow.*, vol. 17, no. 7, pp. 1528–1541, 2024. [Online]. Available: <https://www.vldb.org/pvldb/vol17/p1528-zou.pdf>
- [40] A. Shelmanov, E. Tsymbalov, D. Puzyrev, K. Fedyanin, A. Panchenko, and M. Panov, “How certain is your transformer?” in *Proceedings of the 16th Conference of the European Chapter of the Association for Computational Linguistics: Main Volume, EAACL 2021, Online, April 19 - 23, 2021*, P. Merlo, J. Tiedemann, and R. Tsarfaty, Eds. Association for Computational Linguistics, 2021, pp. 1833–1840. [Online]. Available: <https://doi.org/10.18653/v1/2021.eacl-main.157>
- [41] Z. Sadri, L. Gruenwald, and E. Leal, “Drindex: deep reinforcement learning index advisor for a cluster database,” in *IDEAS 2020: 24th International Database Engineering & Applications Symposium, Seoul, Republic of Korea, August 12-14, 2020*, B. C. Desai and W. Cho, Eds. ACM, 2020, pp. 11:1–11:8. [Online]. Available: <https://doi.org/10.1145/3410566.3410603>
- [42] G. P. Licks, J. M. C. Couto, P. de Fátima Míche, R. D. Paris, D. D. A. Ruiz, and F. Meneguzzi, “Smartix: A database indexing agent based on reinforcement learning,” *Appl. Intell.*, vol. 50, no. 8, pp. 2575–2588, 2020. [Online]. Available: <https://doi.org/10.1007/s10489-020-01674-8>
- [43] T. Siddiqui, S. Jo, W. Wu, C. Wang, V. Narasayya, and S. Chaudhuri, “Isum: Efficiently compressing large and complex workloads for scalable index tuning,” in *Proceedings of the 2022 International Conference on Management of Data, ser. SIGMOD '22*. Association for Computing Machinery, 2022, pp. 660–673.